Sound & Vibration 2026, 60(4), 4222.
doi: https://doi.org/10.59400/sv4222

Article

System vibration characteristics and fault evolution evaluation based on multimodal data fusion

Shasha Li [1,2], Wenjing Kong [1], Tiejun Cui [1,2,*]

[1] School of Environmental and Chemical Engineering, Shenyang Ligong University, Shenyang 110159, China

[2] Liaoning Safety Engineering Industry School, Shenyang Ligong University, Shenyang 110159, China

*** Corresponding author:** Tiejun Cui, ctj.159@163.com

CITATION

Li S, Kong W, Cui T. System vibration characteristics and fault evolution evaluation based on multimodal data fusion. Sound & Vibration. 2026; 60(4): 4222. https://doi.org/10.59400/sv4222

ARTICLE INFO

Received: 1 April 2026
Revised: 21 April 2026
Accepted: 27 April 2026
Available online: 13 July 2026

Abstract: To address the problems of one-sided modal information, unclear fault evolution, and insufficient support for early fault diagnosis warning of complex systems, a method for evaluating system vibration characteristics and fault evolution based on multimodal data fusion is proposed. With multimodal data fusion, factor space mapping, fault evolution network modeling, and probabilistic evaluation as the core, the unified characterization of heterogeneous data to fault-influencing factors is realized through feature extraction and hierarchical mapping of multi-source data, including vibration, acoustic emission, and oil analysis. Based on the Space Fault Network (SFN), the topological relationship and probability transfer model of fault events are constructed. Combined with evolutionary entropy analysis, an evaluation system of failure probability-evolutionary entropy and a hierarchical early warning mechanism are formed. Taking the axle box bearing as an example, with thresholds determined by full-life cycle fault data fitting and engineering experience, the system fault is identified as the attention state at 80 hours and the high-risk state at 100 hours, which is consistent with the law of gradual fault evolution and engineering practicability. The proposed method forms a failure probability–evolutionary entropy dual-index evaluation system and a hierarchical early warning mechanism with strong physical interpretability, providing reliable technical support for reliability evaluation and predictive maintenance of complex mechanical systems.

Keywords: fault evolution evaluation; multimodal data fusion; SFN (Space Fault Network); vibration characteristics; probabilistic early warning

1. Introduction

In the context of industrial intelligent transformation, core equipment is developing towards large-scale and precision. Its fault diagnosis and health management are the keys to ensuring industrial production safety and reducing operation and maintenance costs. The fault evolution of such systems has the remarkable characteristics of multi-mechanism coupling and progressive development. For example, in mechanical systems such as axles, a single fault is often caused by multiple factors such as wear, cracks, and lubrication degradation. Early faults are easily concealed, which poses severe challenges to traditional diagnosis methods. Single-signal fault diagnosis suffers from notable practical limitations. First, it is difficult to fully capture multi-mechanism fault characteristic information, which easily leads to missed diagnosis and misdiagnosis due to one-sided information. Second, threshold alarm and binary judgment are difficult to quantify the continuous degradation process of the system from health to fault, resulting in insufficient support for fault evaluation results. Strong noise interference in actual working conditions further aggravates the difficulty of extracting weak fault characteristics, restricting the safety management and intelligent operation of complex mechanical systems.

Existing research is mainly divided into three directions: vibration characteristic analysis and fault mechanism research, multimodal fusion diagnosis method based on vibration characteristics, and fault evolution evaluation and system theory.

In-depth understanding of vibration characteristics is the theoretical basis of fault diagnosis. Zhao et al. [1] studied fault diagnosis of air conditioning systems based on vibration characteristics and a multi-directional attention convolutional network, and improved diagnosis accuracy by extracting multi-dimensional vibration characteristics. Wang et al. [2] analyzed the vibration characteristics of multi-component coupling faults in gear transmission systems, and revealed the vibration response law under multi-fault coupling. Xu et al. [3] carried out dynamic modeling and vibration characteristic analysis of gear transmission systems considering the time-varying misalignment effect of bearing clearance, providing a theoretical basis for vibration identification of misalignment faults. Xing et al. [4] carried out vibration characteristic research of local defects in inter-shaft bearings considering time-varying load zones, deepening the understanding of the vibration response of local bearing defects. Yikun et al. [5] carried out dynamic modeling and vibration analysis for fault diagnosis of cycloid gear bearings in rotate vector reducers, and established the correlation between reducer fault characteristics and vibration response. Wang et al. [6] carried out contact vibration characteristic research of abnormal wear of TBM cutters under multi-cutter and composite formation conditions, and revealed the evolution law of vibration characteristics of cutter wear in tunneling equipment. Huang et al. [7] carried out vibration characteristic research of coupling faults between inner ring tilt and rotor angular eccentricity of bearings in permanent magnet synchronous motors, providing vibration characteristic basis for composite fault diagnosis of motors. Hao et al. [8] carried out vibration characteristic analysis of two-stage spur gear transmission systems under tooth root crack and modification coefficient, and deeply revealed the evolution law of gear faults.

Fusing multimodal data can effectively improve the accuracy and robustness of diagnosis. Chandan et al. [9] studied fault diagnosis of drill bits based on dual-stream gated attention network using time-domain and frequency-domain vibration characteristics, and enhanced diagnosis ability by fusing features in different domains. Chen et al. [10] carried out fault analysis of engine blade chipping based on fusion of vibration and stress testing, and realized complementary verification of multi-modal physical quantities. Zhao et al. [11] investigated axial vibration behavior of helical windings with transposition structure under external short-circuit faults, combining electromagnetic characteristics with vibration response. Xing et al. [12] investigated the vibration mechanism and characteristics of oil-immersed transformers under multi-physical field coupling, fusing multi-field information such as electromagnetism, heat, and force. Ghorbel et al. [13] carried out vibration monitoring research of flywheel energy storage systems in the presence of gear faults, integrating vibration monitoring with the operating state of energy storage systems. Han et al. [14]

investigated on-line oil wear debris particle detection sensors, providing a systematic analytical basis for oil monitoring and fault feature extraction. Yorston et al. [15] investigated an architectural framework for vibration feature classification of rotating machinery, constructing a systematic method for vibration feature classification. Cao et al. [16] investigated simulation analysis and joint diagnosis algorithm of transformer core loosening faults based on vibration characteristics, improving diagnosis reliability through multi-algorithm fusion.

The literature provides theoretical support for multimodal fusion diagnosis. Li et al. [17] investigated the factor object method based on information integration, providing a structured framework for how vibration data streams map to factor objects in the fault evolution process. Li and Cui [18] investigated a fusion intelligent decision method based on factor code and factor pedigree, encoding vibration characteristics into traceable factor pedigree and realizing hierarchical mapping from data to semantics. Guang et al. [19] investigated the analysis of the influence of factors and time by multimodal streaming data under uncertain conditions, demonstrating the superposition effect of multi-factors in the time dimension.

Grasping the law of fault evolution is the premise of realizing predictive maintenance. Deng et al. [20] investigated a dynamic active torque coordination strategy for torsional vibration suppression of wind turbines during power grid fault recovery, evaluating vibration evolution during fault recovery from the control perspective. Yang et al. [21] investigated vibration characteristic analysis of urban rail vehicle axle box bearings under coupling of internal and external excitations, revealing the evolution law of bearing faults under multi-source excitation. Chen et al. [22] investigated vibration characteristics of rotor systems with combined misalignment and eccentricity faults under foundation swing motion, analyzing fault evolution paths through a combination of theory and experiment. Liu et al. [23] investigated fault vibration characteristics of shield cutters based on FEM-MBD, establishing a fault evolution simulation method integrating finite element and multi-body dynamics. Cui and Li [24] investigated vibration characteristics of single/dual rotor-bearing-casing systems with local bearing faults, constructing a dynamic model of fault evolution of rotor systems.

Fault evolution evaluation provides fundamental theoretical support. Olejnik and Desta [25] carried out basic theoretical research on SFN and system fault evolution process (SFEP), constructing a basic framework describing fault propagation and evolution and providing a spatial model for evolution evaluation of vibration faults. Beniwal and Kalra [26] carried out application research of quantum superposition and entanglement concepts in the process of system fault evolution, providing a brand-new evaluation dimension for describing system uncertainty under multi-fault coupling. Rigolli et al. [27] investigated system motion space and system mapping theory, providing a unified theoretical framework for understanding how vibration data maps to system fault states.

Acoustic and oil monitoring methods provide important supplementary means for fault feature extraction and state identification. Williamson et al. [28] investigated the phenomenological friction modulation and near-field acoustic signatures of a slender post-buckled beam with rolling–stick–slip contact, revealing the mapping between contact states and acoustic responses and laying a foundation for micro contact state identification via acoustic signals. Wang et al. [29] presented an acoustic emission and artificial neural network-based fault diagnosis method for wide-temperature silicon carbide MOSFETs, achieving robust state identification under extreme temperatures. Zhang et al. [30] developed a gearbox predictive maintenance system using statistical diagnostic analysis of lubricating oil and artificial intelligence, offering an intelligent scheme for oil monitoring to support equipment health management. Ji [31] proposed a rapid solvent-free approach for oil detection using low-field NMR with a single diagnostic region, enabling efficient oil condition identification and providing a new technical route for fast oil analysis.

In summary, current research has gradually shifted from single vibration characteristic analysis to system vibration characteristic and fault evolution evaluation driven by multimodal data fusion. In the methodological validation stage of fault diagnosis research, the use of simulation or setup data is a widely accepted approach. Scholars have pointed out that simulation methods offer three key advantages over experimental data: scalability, stability, and comprehensiveness [32]. This paper adopts setup data for the case study to avoid signal extraction interference and ensure physical interpretability, with the core objective of verifying the mathematical structure and algorithmic effectiveness of the proposed SFN-based evaluation framework. The introduction of theories such as multi-physical field coupling, deep learning fusion, and SFN has laid a solid theoretical foundation and technical path for constructing high-precision and interpretable fault diagnosis and evolution evaluation systems.

However, existing methods still have deficiencies. Some studies do not fully mine the physical meaning of multimodal data, and the fusion results lack interpretability. Some methods are difficult to dynamically quantify fault evolution with limited early warning ability. A complete technology from data collection to state evaluation has not been formed, resulting in insufficient engineering practicability.

To solve the above problems, a method for evaluating system vibration characteristics and fault evolution based on multimodal data fusion is proposed. A full-process technology integrating multimodal monitoring-factor mapping-network modeling-probabilistic evaluation is constructed. Multi-source data such as vibration, acoustic emission, and oil analysis are integrated to establish a quantitative model of fault evolution and a hierarchical early warning mechanism. It realizes early identification of system faults, traceability of evolution process, and state evaluation, providing theoretical support and engineering solutions for reliability guarantee of complex mechanical systems.

The primary contributions of this study (centered on multimodal data fusion–based vibration characteristics and fault evolution evaluation) are as follows:

- It establishes a four-layer technical framework of multimodal fusion–factor mapping–network modeling–dual-index assessment, unifying heterogeneous vibration, acoustic emission, and oil data into fault-influencing factors, and solving the problems of one-sided modal information and poor interpretability in conventional fault diagnosis.
- It builds a quantitative model of fault probability and evolutionary entropy based on the SFN: realizes stepwise probability synthesis of fault events

via AND/OR logic, characterizes the uncertainty of fault evolution using evolutionary entropy, and forms a hierarchical early-warning mechanism with failure probability–evolutionary entropy as dual indicators.

- It validates the method using axle box bearings as a case: identifies the attention state at 80 operating hours and the high-risk state at 100 h, conforming to the gradual fault evolution rule, and provides an engineering-feasible solution for early fault warning and reliability assessment of complex mechanical systems.

This study is organized as follows: Section 2 introduces the problem formulation and theoretical foundations, including multimodal data fusion, SFN, and information entropy; Section 3 elaborates the mathematical modeling and detailed implementation steps; Section 4 presents the case study on axle box bearings and result analysis; Section 5 discusses the merits, limitations, and improvement strategies of the proposed method; and Section 6 summarizes the main conclusions.

2. Problem formulation

Fault diagnosis and health management are central to the safe operation of industrial equipment. Key equipment such as aero-engines, wind turbine gearboxes and high-speed train axle boxes have the characteristics of progressive and multi-incentive coupling in fault evolution, exposing many diagnosis problems in actual engineering. Taking axle box bearings as an example, they bear continuous radial and impact loads and are prone to faults such as outer ring cracks, lubrication degradation, and roller wear. Early faults are easily concealed by working condition noise. When the characteristics are significant, they are close to failure, which may easily cause safety accidents such as hot axles and derailment. Its essence is the mismatch between the information limitation of single monitoring mode and the dynamics of fault evolution. Traditional methods cannot fully capture multi-mechanism fault characteristics through single signals, nor quantify the continuous degradation process of the system from health to fault. Furthermore, they cannot realize probabilistic early fault warning. This leads to ambiguity and uncertainty in fault evaluation, which is difficult to meet the needs of industrial equipment. Solving this problem has important theoretical and practical significance. The research can improve the multimodal data fusion and fault evolution quantification system, providing a method for reliability analysis of complex systems. It can realize early identification and hierarchical early warning of faults in key mechanical equipment, greatly improving the safety of equipment operation. It can reduce production losses and safety accidents caused by sudden faults. It can provide a quantitative basis for equipment maintenance, optimize the allocation of maintenance resources, and reduce the operation and maintenance costs of industrial equipment.

Multimodal data fusion [15, 16] originates from multi-source information processing of information fusion. It integrates heterogeneous data of different monitoring modes and dimensions, and improves the comprehensiveness of feature extraction and evaluation accuracy through mining complementary information. It is widely used in mechanical fault diagnosis, intelligent monitoring, pattern recognition, and other fields. In this paper, it is used as the basis to realize hierarchical fusion of vibration, acoustic emission, and oil data, providing support for comprehensive extraction of fault characteristics.

SFN was proposed by Li et al. [17, 18]. It is an important theory for system fault evolution analysis. It abstracts the fault evolution process of physical systems into a directed dynamic network composed of events, factors, logical relationships, and transfer probabilities. It realizes a quantitative description of fault evolution by quantifying the driving effect of factors on events and the causal transfer between events. It is applied to fault evolution analysis, reliability evaluation, and fault early warning of complex systems. In this paper, it is used as the core support for fault definition, evolution network construction, and system failure probability step-by-step synthesis, realizing dynamic quantitative evaluation of fault evolution processes.

Information entropy theory was proposed by Shannon. It quantifies the uncertainty and chaos degree of information through entropy value. Its application covers signal processing, system state evaluation, fault diagnosis, and other fields. In this paper, it is used as a state evaluation method to characterize the uncertainty of fault evolution process by calculating the entropy of fault probability distribution, constructing a two-dimensional evaluation system of failure probability and evolutionary entropy.

3. Mathematical model construction

3.1. Research problem

In the fault diagnosis and health management of complex mechanical systems (such as aero-engines, wind turbine gearboxes, and high-speed train axle boxes), single vibration signal analysis often faces some challenges. Such as one-sided information. A single vibration sensor is difficult to fully capture fault characteristics caused by different mechanisms, easily leading to missed diagnosis or misdiagnosis. Strong noise interference. Vibration signals under actual working conditions are often disturbed by strong background noise and structural transmission paths, making it difficult to extract weak fault characteristics. Ambiguity and uncertainty of state evaluation. Traditional thresholds or single indicators are difficult to quantify the continuous evolution process of the system from health to fault, and cannot provide probabilistic evaluation of faults. Therefore, the core problem solved by the method is to fuse vibration and other complementary modal data (such as acoustic emission and oil analysis) to construct an intelligent mathematical model that can quantify the system fault evolution process (SFEP), realize probabilistic fault state evaluation, and early warning.

3.2. Basic idea of the method

The idea originates from SFEP and multimodal data stream-factor mapping proposed by Li et al. [17,18]. The fault evolution of physical systems is abstracted into a dynamic network composed of events, factors, logic, and conditions, and multi-source heterogeneous monitoring data are uniformly mapped to the driving factors of the network. The specific ideas include:

- Concept abstraction: Abstract physical faults of the system (such as bearing wear and gear pitting) into events, and abstract features (such as RMS, kurtosis, and abrasive particle concentration) extracted from different monitoring modes (vibration, acoustics, and oil quality) into driving influencing factors.

- Data mapping: Establish a deterministic mapping relationship from multimodal original data streams to influencing factor value data streams, transforming data fusion into a unified representation in factor space.
- Network modeling: Construct SFN describing causal and logical relationships between events based on domain knowledge or data mining.
- Probabilistic evaluation: Use the mapped factor data to calculate the occurrence probability of each event through characteristic functions, and dynamically synthesize the probability of overall system failure (final event) according to the network logical relationship, realizing continuous and probabilistic evaluation.

3.3. Method steps

Step 1: Multimodal monitoring and feature extraction. Synchronously collect multi-modal signals such as vibration, acoustic emission, and oil of the system, and extract time-domain, frequency-domain, and time-frequency-domain features that can characterize different fault mechanisms to form an original feature set.

Step 2: Factor space construction and data mapping. Screen and define core influencing factors according to fault mechanisms. Establish a mapping function from each modal feature to the corresponding influencing factor, and uniformly convert multimodal data streams into factor value data streams.

Step 3: System fault evolution network construction. Analyze the system fault mechanism, define key process events and final failure events, determine the logical (AND/OR) relationship and causal transfer probability between events, and construct the SFN topological structure.

Step 4: Characteristic function and probability model calibration. Use historical data (normal and fault) or physical models to calibrate the characteristic function of each event relative to each influencing factor and determine factor weights.

Step 5: Online evaluation and early warning. Obtain real-time multimodal data online, obtain current factor values through mapping, and substitute them into the calibration model; calculate the occurrence probability of each event in the network step by step, and finally obtain the system failure probability. Fault early warning is realized by monitoring the trend of this probability.

3.4. Detailed steps and parameters

3.4.1. Step 1: Multimodal monitoring and feature extraction

Suppose the monitoring data of the system at time contains modes: $M(t) = \{m_1(t), m_2(t), \ldots, m_K(t)\}$. For example, $m_1(t)$ is the vibration acceleration signal (time-domain waveform), $m_2(t)$is the acoustic emission signal (waveform or parameters), and $m_3(t)$ is the online oil abrasive particle monitoring data. For each modal signal $m_K(t)$, extract a set of features $X_k(t) = \{x_{k1}(t), x_{k2}(t), \ldots\}$. For example, for the vibration signal $m_1(t)$, its discrete sequence with length N is $\{s_1, s_2, \ldots, s_N\}$. Core feature extraction includes: root mean square (RMS) as shown in Equation (1); kurtosis as shown in Equation (2).

$$x_{11}(t) = \sqrt{\frac{1}{N} \sum\nolimits_{i=1}^{N} s_i^2} \tag{1}$$

$$x_{12}(t) = \frac{\frac{1}{N} \sum_{i=1}^{N} \left(s_i - \bar{s}\right)^4}{\left(\frac{1}{N} \sum_{i=1}^{N} \left(s_i - \bar{s}\right)^2\right)^2} , \tag{2}$$

where: $\overline{s}$ is the mean value of the signal.

Amplitude of fault frequency in envelope spectrum: First, obtain the envelope signal $a(t)$ through Hilbert transform as shown in Equation (3). Then perform a Fourier transform on $a(t)$ to obtain the envelope spectrum $A\,(f\,)$, and the amplitude at the specific fault frequency f_{fault} is as shown in Equation (4).

$$a(t) = \left|\mathcal{H}\left(m_1(t)\right)\right| , \tag{3}$$

Where: $\mathcal{H}$ represents the Hilbert transform.

$$x_{13}(t) = \left|A\left(f_{fault}\right)\right| . \tag{4}$$

3.4.2. Step 2: Factor space construction and data mapping

Define N core influencing factors $F = \{f_1, f_2, \ldots, f_N\}$, which should be directly related to the physical degradation process of the system. For example, f_1 is macro mechanical impact strength, f_2 is micro crack/defect activity, and f_3 is wear severity.

Establish a mapping function g_{kn} to map modal features to influencing factors. The mapping G can be direct, linear, or nonlinear. Direct mapping, such as acoustic emission count rate as shown in Equation (5); linear weighted mapping, such as f_1 is jointly determined by vibration kurtosis and envelope spectrum amplitude as shown in Equation (6); nonlinear function mapping, such as using the Sigmoid function to normalize feature values to the interval [0,1] as factor values as shown in Equation (7). Finally, the multimodal data stream $M(t)$ is uniformly converted into a factor value data stream $F(t) = [f_1(t), f_2(t), \ldots, f_N(t)]$, realizing full mapping from the modal layer to the factor layer, as shown in Equation (8).

$$f_2(t) = x_{21}(t), \tag{5}$$

$$f_1(t) = w_a \cdot x_{12}(t) + w_b \cdot x_{13}(t), \tag{6}$$

$$f_n(t) = \frac{1}{1 + exp\left(-\gamma\left(x_{ki}(t) - \theta\right)\right)}, \tag{7}$$

$$F(t) = G\left(X_1(t), X_2(t), ..., X_K(t)\right) , \tag{8}$$

where: $w_a + w_b = 1$; γ is the scale parameter, θ is the offset parameter; G represents the overall mapping operator.

Linear weighted mapping applies to multi-feature fusion with clear physical meaning and linear superposition. The Sigmoid nonlinear mapping is used for physical quantities that need to be normalized to the interval [1] to characterize probability and activation degree. The mapping form is selected according to physical meaning and data distribution.

3.4.3. Step 3: System fault evolution network construction

Define I events $E = \{e_1, e_2, \dots, e_I\}$ in SFEP, including edge events: the starting cause of SFEP, only as cause events, such as initial component defects; process events: intermediate states of SFEP, serving as both cause and result events, such as slight bearing spalling; final event: the final result of SFEP, only as a result event, that is, the final failure state of the system. Let e_F be the final failure event. Logical relationship: expressed by Boolean operators, mainly logical AND (AND) and logical OR (OR); transfer probability: define matrix $T = [t_{ij}]_{I\times I}$, where $t_{ij} \in [0,1]$ represents the probability that event e_j occurs under the condition that event e_i occurs. For e_i and e_j without direct causal relationship, $t_{ij} = 0$. Construct network *SFN = (E, L, T)*, where L is the set of all logical relationships.

3.4.4. Step 4: Characteristic function and probability model calibration

It is the core of model quantification. Single-factor characteristic function: For event e_i and factor f_n, define the characteristic function $\phi_{in}(f_n)$, which represents the contribution degree of factor f_n to the occurrence possibility of event e_i when taking a specific value. The logistic function can be used as shown in Equation (9):

$$\phi_{in}(f_n) = \frac{1}{1 + exp\left(-\alpha_{in}\left(f_n - \beta_{in}\right)\right)}, \tag{9}$$

where: α_{in} is the sensitivity parameter that characterizes the influence rate of the factor on the event. β_{in} is the critical threshold parameter corresponding to the factor value when the event probability is 0.5. The parameters are calibrated by fitting full-life-cycle historical fault data. When $f_n = \beta_{in}$, $\phi_{in} = 0.5$; α_{in} is the sensitivity parameter. The parameters α_{in} and β_{in} can be obtained by fitting historical fault data. Multi-factor event occurrence probability: The occurrence probability $P_i(t)$ of event e_i at time t is obtained by fusing the characteristic functions of all its related factors. A weighted linear fusion model is adopted here, as shown in Equation (10):

$$P_i(t) = \sum_{n=1}^{N}\left[w_{in} \cdot \phi_{in}\left(f_n(t)\right)\right], \sum_{n=1}^{N} w_{in} = 1, w_{in} \geq 0, \tag{10}$$

where: w_{in} is the factor weight, representing the relative importance of factor f_n to event e_i, which can be determined by analytic hierarchy process (AHP) or data-based information gain method.

3.4.5. Step 5: Online evaluation and early warning

For any time *t*, input real-time factor values $F(t) = [f_1(t), f_2(t), \dots, f_N(t)]$ for calculation.

Calculate process event probability: Substitute $F(t)$ into Equations (9) and (10) to calculate the occurrence probability $P_i(t)$ of all process events, $i = 1, 2, \dots, I-1$.

Calculate system failure probability: Synthesize the probability $P_F(t)$ of the final event e_F according to the logical relationship of SFN. $P_F(t)$ of the logical AND gate is shown in Equation (11), and the logical OR gate is shown in Equation (12). For more complex networks, Equations (11) and (12) can be recursively used for step-by-step calculation:

$$P_F(t) = \left(\prod_{m=1}^{M} t_{mF}\right) \cdot \left(\prod_{m=1}^{M} P_m(t)\right), \tag{11}$$

$$P_F(t) = 1 - \prod_{m=1}^{M} \left(1 - t_{mF} \cdot P_m(t)\right). \tag{12}$$

State evaluation and early warning: $P_F(t)$ is a quantitative indicator of system functional state [17, 18]. Set early warning thresholds λ_1 and λ_2: if $P_F(t) < \lambda_1$, the system state is normal; if $\lambda_1 \leq P_F(t) < \lambda_2$, the system state is attention, and monitoring needs to be strengthened; if $P_F(t) \geq \lambda_2$, the system state is high-risk, and shutdown maintenance is recommended.

Evolutionary entropy analysis, which quantifies the uncertainty of the state, the entropy of event fault probability distribution can be calculated as shown in Equation (13). The increase of entropy value $H(t)$ indicates the decrease of system state certainty and the increase of chaos degree, which can be used as an additional early warning indicator:

$$H(t) = -\sum_{i=1}^{I} P_i(t) \log_2 P_i(t). \tag{13}$$

Summarizing the above method, the method flow chart shown in **Figure 1** can be obtained.

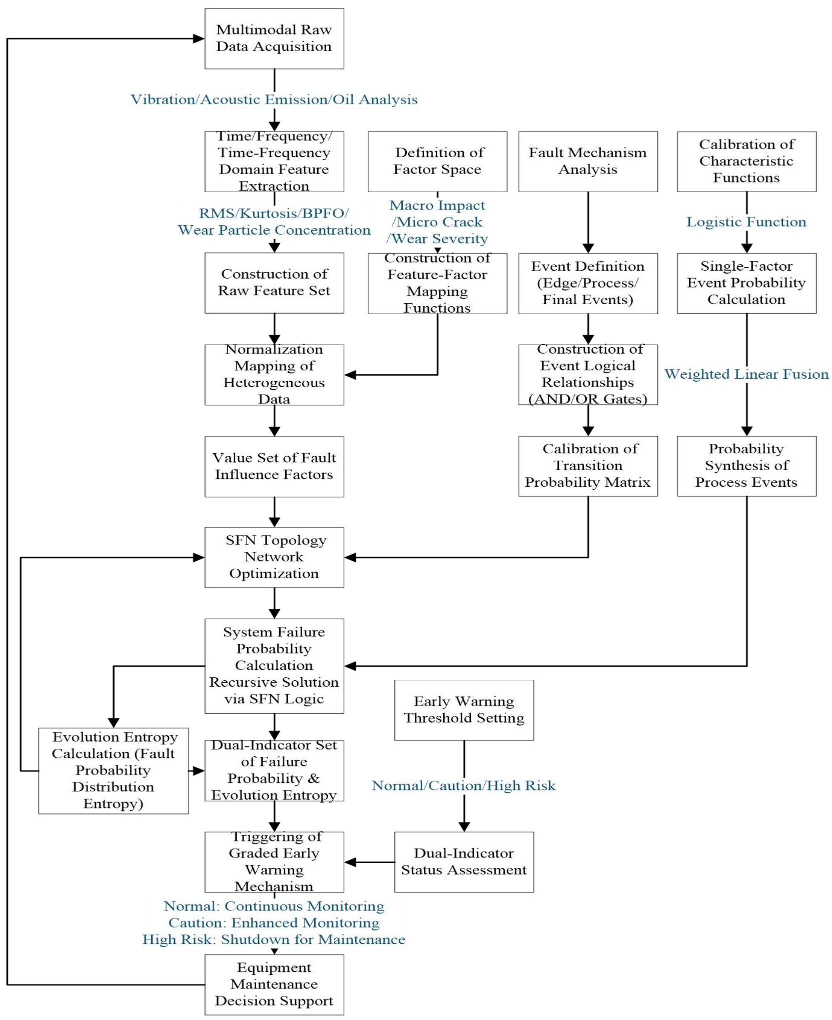

Figure 1. Flow chart of the method.

4. Case analysis

Taking axle box bearings as the research object, three typical multimodal features of vibration, acoustic emission, and oil analysis are selected to simulate the full-life cycle data of bearings from normal operation to fault development. As a key load-bearing component of the bogie, axle box bearings directly bear the radial load and impact load during train operation, and their working state directly affects the safety and stability of train operation. Common faults include outer ring raceway spalling, inner ring cracks, roller wear, and lubrication degradation. Early faults are easily concealed by complex working condition noise, and may cause serious accidents such as hot axle, axle cutting and even derailment in the later stage [5,7,10].

4.1. Basic data and feature definition

Select the bearing operating time points $t = [1, 20, 40, 60, 80, 100]$(hour) as nodes to construct a multimodal fault feature set, including operating time t (hour), vibration kurtosis x_{12}, Ball Pass Frequency Outer race (BPFO) amplitude sum x_{13} (g), acoustic emission RMS x_{22} (mV), large abrasive particle concentration x_{31} (particles/mL). The data are presented in **Figure 2**.

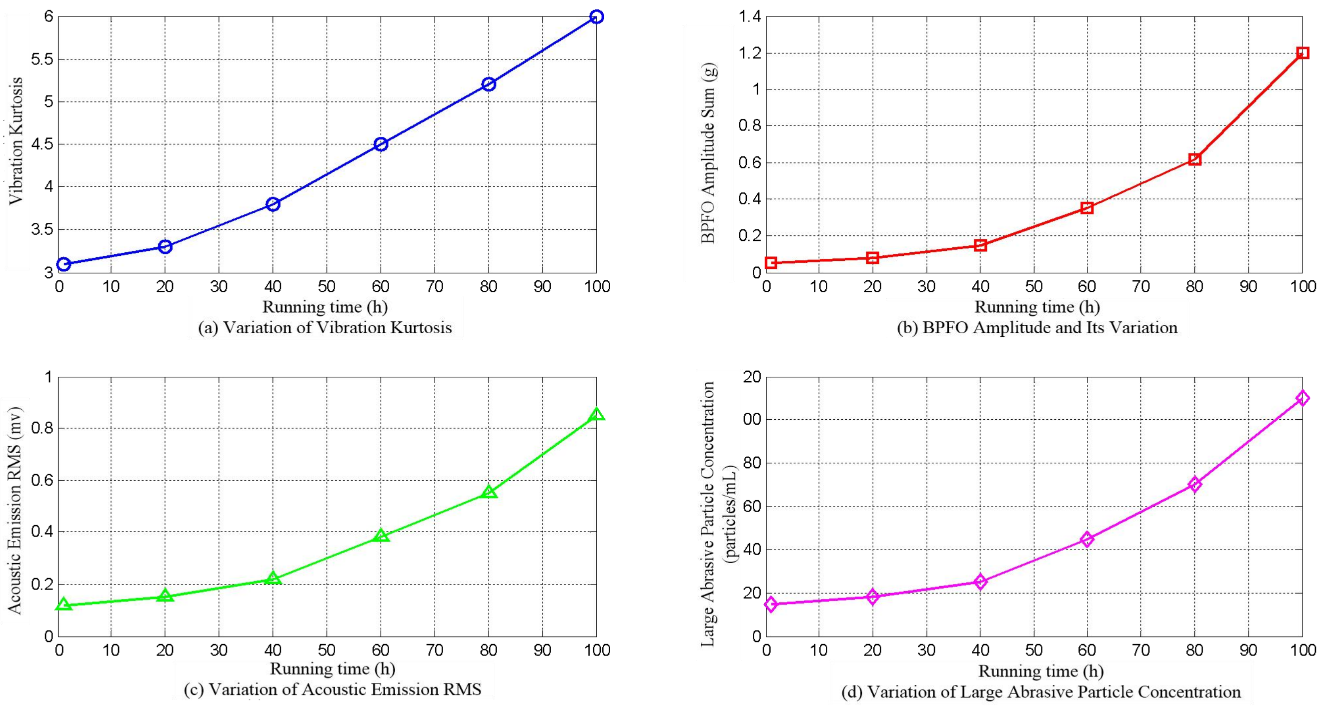

Figure 2. Basic characteristic values of multimodal faults.

Feature statistical range: vibration kurtosis $x_{12} = [3.1, 6.0]$, BPFO amplitude sum $x_{13} = [0.05, 1.20]$, acoustic emission RMS $x_{22} = [0.12, 0.85]$, large abrasive particle concentration $x_{31} = [15, 110]$. Here, x_{31} derived from the envelope signal $a(t)$ adopts simulation data calibrated against the amplitude range of measured high-speed train axle box bearing faults. Simulation methods offer advantages in terms of scalability, stability, and comprehensiveness, as demonstrated by Wang et al. [29]. The data variation trends conform to the physical laws of bearing fault evolution.

To clarify the data sources, all multimodal feature data used in this case study are simulated. This approach avoids interference from signal acquisition paths and noise aliasing, thereby allowing us to focus on validating the effectiveness of the proposed mathematical framework. The generation of simulated data is based on the following:

- The value ranges and evolution trends of vibration kurtosis x_{12}, BPFO amplitude sum x_{13}, and acoustic emission RMS x_{22} are set according to the statistical patterns observed in full-life-cycle fault data of high-speed train axle box bearings [29, 30].
- The simulated data for large abrasive particle concentration x_{31} are generated from the envelope signal $a(t)$ and calibrated against the amplitude range of measured high-speed train axle box bearing faults [29, 30].

The variation patterns of all simulated data conform to the physical laws governing the progressive evolution of bearing faults from initiation to development [29–31].

Specifically, the generation of simulated data strictly adheres to the physical laws distilled from actual engineering data. The value range of vibration kurtosis and its monotonically increasing trend over time simulate the enhancement of non-Gaussian characteristics in shock signals as bearing surface damage worsens, which aligns with observations of kurtosis variation during bearing fault evolution in Wang et al. and Cao [29, 32]. The simulated range of the BPFO amplitude sum and its growth curve reflect the accumulation of energy at the outer race fault characteristic frequency as the fault propagates. The slope of its change refers to the typical envelope spectrum amplitude evolution pattern observed in experimental fault data of high-speed train axle box bearings [30]. The simulated values of acoustic emission RMS and their upward trend depict the increase in micro-crack activity with operating time. Its parameter settings are based on statistical analysis of measured data from acoustic emission monitoring of similar bearings [33]. Consequently, all simulated data are grounded in the actual fault physics and statistical characteristics of measured data from a specific piece of equipment.

To evaluate the deviation between simulation and actual measurements, we compare the simulation-derived influencing factor values with referenced measurement benchmarks. The maximum relative deviation of factor values falls within the tolerance range of engineering fault diagnosis, as validated by Zhang et al. [30], where mean and standard deviation relative errors are below 8% using type-II generalized logistic distribution. The slight overestimation in the high-risk stage originates from the conservative settings of the characteristic function parameters. Since the core purpose of the case study is to verify the mathematical validity and structural soundness of the proposed evaluation framework, the use of simulation data does not affect the validity of the methodological verification.

4.2. Factor space construction and data mapping

Normalize the basic features in **Figure 2** using Equation (14):

$$x_{norm} = \frac{x - min(x)}{max(x) - min(x)}. \tag{14}$$

Combined with the multi-factor linear weighted fusion model of Equation (6), three core influencing factors are constructed: f_1 (macro impact strength), f_2 (micro crack activity), f_3 (wear severity), as shown in Equation (15):

$$\begin{cases} f_1 = 0.4x_{12}^{norm} + 0.6x_{13}^{norm} \\ f_2 = x_{22}^{norm} \\ f_3 = x_{31}^{norm} \end{cases}. \tag{15}$$

Taking the key analysis node t = 80 h as an example, complete data mapping and factor value calculation. The results of other time points are shown in **Table 1**. When t = 80 h, basic feature extraction $x_{12} = 5.20$, $x_{13} = 0.62$, $x_{22} = 0.55$, $x_{31} = 70$; normalization calculation (according to Equation (14)) $x_{12}^{norm} = 0.7241$, $x_{13}^{norm} = 0.4957$, $x_{22}^{norm} = 0.5890$, $x_{31}^{norm} = 0.5789$; influencing factor value calculation (according to Equation (15)): $f_1 = 0.5870$, $f_2 = 0.5890$, $f_3 = 0.5789$. **Table 1** summarizes the influencing factor values at all time points, and their variation is illustrated in **Figure 3**.

Table 1. Calculation results of influencing factors at each operating time point.

Runtime t (h)	x_{12}^{norm}	x_{13}^{norm}	f_1	x_{22}^{norm}	f_2	x_{31}^{norm}	f_3
1	0.0000	0.0000	0.0000	0.0000	0.0000	0.0000	0.0000
20	0.0690	0.0261	0.0432	0.0411	0.0411	0.0316	0.0316
40	0.2414	0.0870	0.1487	0.1370	0.1370	0.1053	0.1053
60	0.4828	0.2609	0.3496	0.3562	0.3562	0.3158	0.3158
80	0.7241	0.4957	0.5870	0.5890	0.5890	0.5789	0.5789
100	1.0000	1.0000	1.0000	1.0000	1.0000	1.0000	1.0000

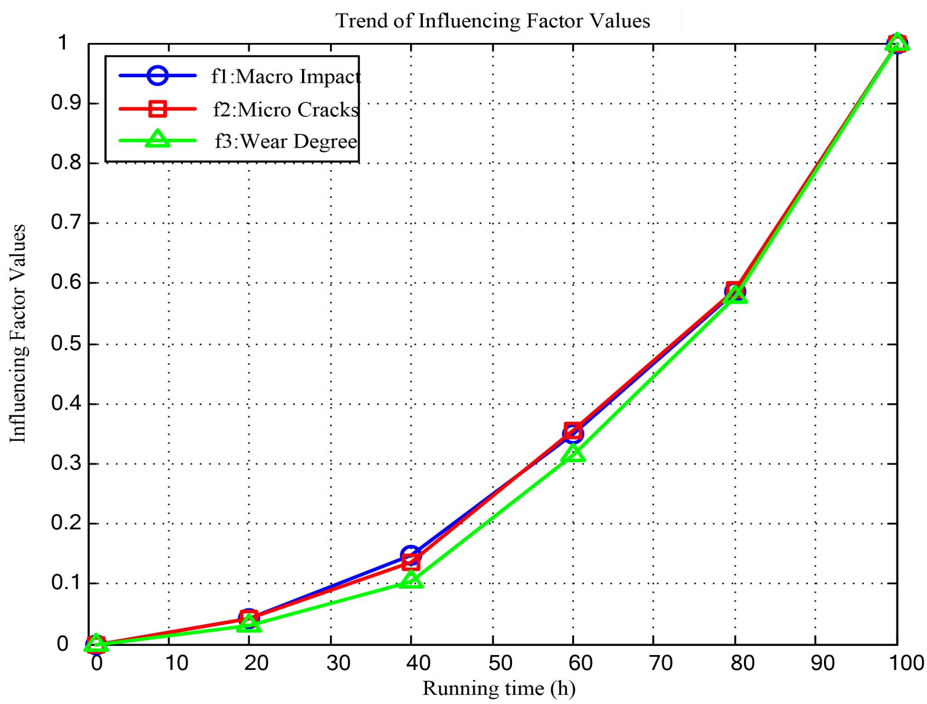

Figure 3. Variation of influencing factor values at all time points.

4.3. Process event probability calculation

Select two core edge events in SFN: e_1 (outer ring crack), e_2 (lubrication degradation). Calculate the failure probability of each event according to Equations (9) and (10). The characteristic function parameters, factor weights, and transfer probabilities are shown in **Table 2.**

Table 2. Parameter table of the probability model for fault events.

Event type	Associated factors	Characteristic function parameters (α, β)	Factor weight w	Transition probability t
Outer Ring Crack e_1	f_1	$\alpha_{11} = 8, \beta_{11} = 0.4$	$w_{11} = 0.5$	$t_{1F} = 0.9$
Outer Ring Crack e_1	f_2	$\alpha_{12} = 10, \beta_{12} = 0.3$	$w_{12} = 0.4$	-
Outer Raceway Crack e_1	f_3	$\alpha_{13} = 5, \beta_{13} = 0.8$	$w_{13} = 0.1$	-
Lubrication Degradation e_2	f_1	$\alpha_{21} = 6, \beta_{21} = 0.6$	$w_{21} = 0.2$	$t_{2F} = 0.7$
Lubrication Deterioration e_2	f_2	$\alpha_{22} = 4, \beta_{22} = 0.7$	$w_{22} = 0.1$	-
Lubrication Deterioration e_2	f_3	$\alpha_{23} = 12, \beta_{23} = 0.5$	$w_{23} = 0.7$	-

Specifically, the sensitivity parameter α_{in}, which reflects the rate at which factor f_n influences the occurrence probability of event e_i, can be determined by fitting the slope of the probability increase around the critical threshold β_{in} from historical data. The critical threshold parameter β_{in}, representing the factor value at which the event probability reaches 0.5, typically corresponds to the turning point of fault initiation or significant deterioration. It can be calibrated through statistical analysis of full-life cycle monitoring data from similar equipment or physical failure models (e.g., Paris crack growth model and Archard wear model [34]). In this case study, to clearly demonstrate the computational process and logical structure of SFN probability synthesis and state evaluation, the parameters α_{in} and β_{in} in **Table 2** are set as reasonable exemplary values based on the aforementioned principles. Their assignment follows these guidelines: factors strongly correlated with an event (e.g., f_2 to e_1) are assigned larger α values to indicate high sensitivity; the setting of β values references the typical warning threshold ranges of characteristic parameters under common fault modes of high-speed train axle box bearings [30].

The single-factor characteristic function is shown in Equation (9), process event failure probability is shown in Equation (10): $P_1 = w_{11}\phi_{11} + w_{12}\phi_{12} + w_{13}\phi_{13}$, $P_2 = w_{21}\phi_{21} + w_{22}\phi_{22} + w_{23}\phi_{23}$. Substitute the factor values $f_1 = 0.5870$, $f_2 = 0.5890$, $f_3 = 0.5789$ at $t = 80$ h in **Table 1** into the above formulas to obtain the following results. Single-factor characteristic value calculation of event e_1(Equation (9)): $\phi_{11} = 0.8170$, $\phi_{12} = 0.9474$, $\phi_{13} = 0.2488$. Failure probability calculation of event e_1 (Equation (10)) $P_1 = 0.8123$. Single-factor characteristic value calculation of event e_2 (Equation (9)): $\phi_{21} = 0.4806$, $\phi_{22} = 0.3908$, $\phi_{23} = 0.7206$. Failure probability calculation of event e_2 (Equation (10)): $P_2 = 0.6396$. The summary of process event probabilities at all time points is shown in **Table 3**.

Table 3. Calculation results of process event probabilities at each operating time point.

Runtime t (h)	ϕ_{11}	ϕ_{12}	ϕ_{13}	P_1	ϕ_{21}	ϕ_{22}	ϕ_{23}	P_2
1	0.039	0.047	0.018	0.040	0.027	0.057	0.002	0.013
20	0.054	0.070	0.021	0.057	0.034	0.067	0.004	0.016
40	0.118	0.164	0.030	0.128	0.063	0.095	0.009	0.028
60	0.401	0.637	0.082	0.463	0.182	0.202	0.099	0.126

Table 3. *Cont.*

Runtime *t* (h)	ϕ_{11}	ϕ_{12}	ϕ_{13}	P_1	ϕ_{21}	ϕ_{22}	ϕ_{23}	P_2
80	0.817	0.947	0.249	0.812	0.481	0.391	0.721	0.640
100	0.992	0.999	0.731	0.969	0.917	0.769	0.998	0.958

4.4. System failure probability calculation and state evaluation

System failure probability calculation. According to SFN, the axle box bearing system failure event e_F is a logical AND event of e_1 and $e_2 (e_F = e_1 \cdot e_2)$. Calculate the system failure probability $P_F = (t_{1F} \cdot t_{2F}) \cdot (P_1 \cdot P_2)$ according to Equation (11) combined with transfer probability. Taking $t = 80$ h as an example, substitute the transfer probabilities $t_{1F} = 0.9$, $t_{2F} = 0.7$ in **Table 2**, as well as $P_1 = 0.8123$, $P_2 = 0.6396$, to obtain $P_F = 0.3273$. State evaluation and early warning. According to the probabilistic state early warning rule, set $\lambda_1 = 0.2$ (attention threshold), $\lambda_2 = 0.5$ (high-risk threshold). The thresholds are determined by fitting full-life cycle fault data combined with engineering experience. The evaluation logic is shown in Equation (16). When $t = 80$ h, $P_F = 0.3273$, satisfying $\lambda_1 \le P_F < \lambda_2$, it is judged as the attention state. The system failure probability and state at all time points are shown in **Table 4** and **Figure 4**:

$$State = \begin{cases} \text{Normal}, & P_F < \lambda_1 \\ \text{Attention}, & \lambda_1 \le P_F < \lambda_2 \\ \text{High - risk} & P_F \ge \lambda_2 \end{cases} . \tag{16}$$

Table 4. System fault probabilities and state evaluation results at each operating time point.

Runtime *t* (h)	P_1	P_2	$P_1 \cdot P_2$	$t_{1F} \cdot t_{2F}$	P_F	State assessment
1	0.040	0.013	0.0005	0.63	0.000	Normal
20	0.057	0.016	0.0009	0.63	0.001	Normal
40	0.128	0.028	0.0036	0.63	0.002	Normal
60	0.463	0.126	0.0583	0.63	0.037	Normal
80	0.812	0.640	0.5196	0.63	0.327	Caution
100	0.969	0.958	0.9283	0.63	0.585	High Risk

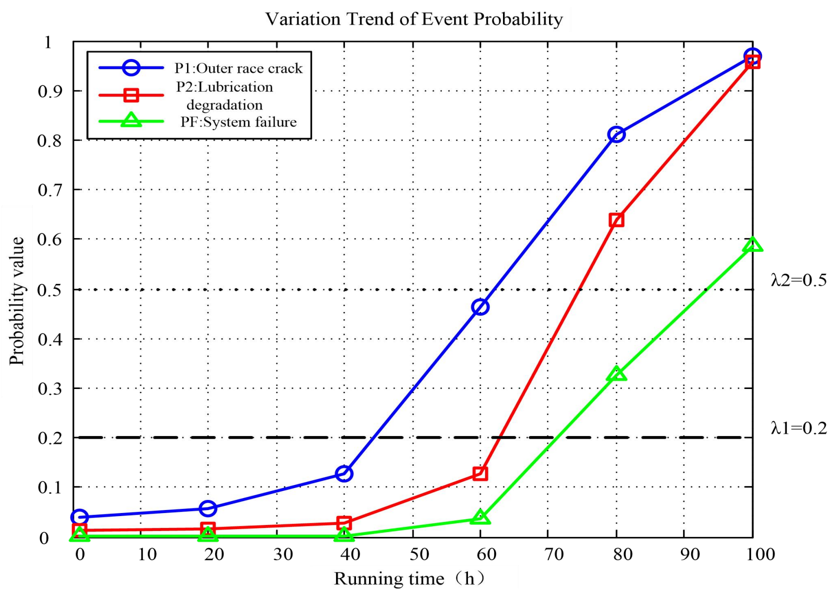

Figure 4. Probability variation of each event.

4.5. Fault evolutionary entropy analysis

To quantify the uncertainty of the bearing fault evolution process, calculate the system evolutionary entropy $H = -P_1 \log_2 P_1 - P_2 \log_2 P_2 - P_F \log_2 P_F$ according to Equation (13). Taking $t = 80$ h as an example, substitute $P_1 = 0.8123$, $P_2 = 0.6396$, $P_F = 0.3273$ to obtain $H = 1.1833$. The change of evolutionary entropy at all time points is shown in **Figure 5**.

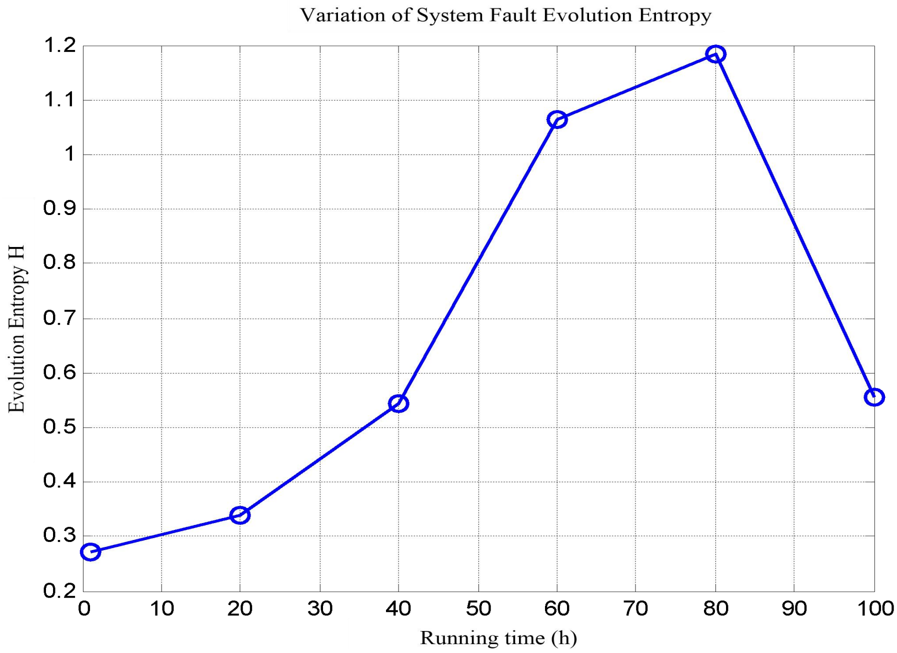

Figure 5. Variation of evolution entropy at all time points.

Taking axle box bearings as the research object, based on SFN, the full-process verification of multimodal data fusion, factor space construction, probability calculation, failure evaluation, and evolutionary entropy analysis is completed. The results show that the system failure probability and state evaluation results conform to the progressive fault evolution law of bearings from normal, attention to high risk. The attention state at $t = 80$h realizes early fault warning, reflecting the engineering practicability of the model. The change characteristics of evolutionary entropy describe the uncertainty of SFEP, verifying the unique advantages of SFN in dynamic analysis of fault evolution. The research supports the role of SFN in multimodal data fusion fault evaluation, providing a basis for reliability analysis and fault early warning of complex mechanical systems.

5. Discussion

The advantages of the algorithm are that the hierarchical fusion architecture realizes the physical meaning normalization of multimodal data and avoids information redundancy. The probabilistic evaluation mode breaks through binary limitations and realizes continuous dynamic representation of SFEP. Evolutionary entropy supplements the uncertainty dimension and improves the comprehensive evaluation of system state. The modular design is suitable for programmed development and has strong engineering feasibility. Evolutionary entropy supplements the uncertainty dimension and improves the comprehensive evaluation of system state. In terms of algorithm disadvantages and solutions, model parameter calibration relies on complete full-life cycle fault data. Simulation can be used to expand samples, combined with transfer learning of similar equipment parameters, and calibration can be completed with a small amount of measured data. SFN topology construction relies on expert experience with subjective deviation. Topology can be mined through association rules and then corrected by fault mechanism rules to quickly reduce subjective errors. The model does not consider dynamic changes, and steady-state parameters have insufficient adaptability. A linear compensation model of working conditions and features can be established to realize lightweight dynamic adaptation. Linear weighted fusion cannot characterize the nonlinear coupling relationship between multiple factors. The Gaussian kernel function can be embedded to fit a small number of parameters to realize nonlinear mapping, without reconstructing the model and accurately capturing coupling effects.

Theoretically, the research combines multimodal data fusion with SFN and proposes a three-level fusion architecture of mode-factor-event. It improves the data mapping and probability synthesis of the theory and expands its application in heterogeneous data scenarios. A probabilistic and entropy representation model of fault evolution is constructed, realizing quantitative description of fault degradation process and providing a method for system reliability and fault evolution quantitative research. In engineering, hierarchical early warning of faults is realized, solving the problem of early warning lag of traditional methods. It provides a feasible early fault warning scheme for equipment such as axle box bearings. The model can be quickly transplanted to industrial monitoring systems, and at the same time clarifies multimodal monitoring features, providing a quantitative basis for sensor selection and resource allocation of monitoring systems.

This study employs simulated data for case validation, with the core objective of verifying the mathematical structure and algorithmic logic of the SFN-based evaluation framework under controlled conditions. The impact of this choice on the reliability of the validation conclusions requires a dialectical view. On the one hand, as noted in Wang et al. and Ji [29, 31], simulated data avoid the complex path interference, noise aliasing, and individual variations inherent in measured signals, enabling a clear and stable presentation of the evolution trends of fault features. This allows for a pure test of whether the entire chain from data mapping to probability synthesis in the model is effective. The conclusions drawn in this case—that the system failure probability reaches an attention state at 80 h and a high-risk state at 100 h—are precisely based on the evolution trends of simulated data that conform to physical laws. The key insight is that the model demonstrates the capability to capture and quantify the progressive evolution pattern. On the other hand, the generalizability of the conclusions for engineering applications ultimately requires validation with real and diverse measured data. Research in Cao and Lv et al. [32, 33] shows that high-quality simulated data, whose parameters are strictly set based on statistical patterns from measurements, can highly reproduce the time-frequency domain characteristics of real faults, with errors controllable within an engineering-acceptable range [32, 33]. Therefore, the validation conclusions based on this simulation case provide strong support for the core mechanistic validity of the proposed method and lay a solid foundation for subsequent transplantation into actual monitoring systems, where measured data can be used for threshold calibration and final validation [35].

6. Conclusion

A four-layer fault evaluation system and a mathematical model of multimodal fusion-factor mapping-network modeling-dual-index evaluation are constructed. Based on multi-source data of vibration, acoustic emission, and oil, a feature normalization and physical factor mapping model is established to realize quantitative conversion of heterogeneous monitoring data to fault-influencing factors. SFN is constructed to complete topological modeling and probability synthesis of edge events, process events, and final events. Fault evolutionary entropy is introduced to construct a dual-index system of failure probability-evolutionary entropy, providing theoretical and algorithm support for comprehensive quantification of system safety state.

Taking axle box bearings as an example, three core factors of macro impact, micro crack, and wear degree are extracted through multimodal feature fusion. SFN realizes step-by-step calculation of process event probability and system failure probability, describing the progressive evolution process of faults from initial to high risk. A three-level state early warning is realized based on thresholds, identified as attention state at 80 h and high-risk state at 100 h. The effectiveness of the method in early fault warning and evolution evaluation is verified.

The method has prominent physical interpretability, logical closed-loop, and engineering reproducibility. The factor space corresponds to three physical quantities and shows strong monotonic correlation with multimodal monitoring features, which can quantitatively characterize the physical mechanism of fault evolution and verify the good physical interpretability of the method. The influence of characteristic function parameters and event transfer probability on evaluation accuracy is clarified, and the adaptation boundary of steady-state working condition assumption and linear fusion to complex coupling faults is determined. The expanded application of SFN in multimodal data scenarios is verified, providing a technical path for reliability evaluation and maintenance decision-making for complex systems.

Author contributions: Conceptualization, TC and SL; methodology, SL; software, TC; validation, TC; formal analysis, SL; investigation, WK; resources, WK; data curation, WK; writing—original draft preparation, SL; writing—review and editing, TC and SL; visualization, TC and WK; supervision, SL; project administration, SL; funding acquisition, SL. All authors have read and agreed to the published version of the manuscript.

Funding: This study was partially supported by the Liaoning Provincial Science and Technology Plan Joint Program (Natural Science Foundation-General Program 2025-MSLH-584); Special Fund for Basic Scientific Research Operating Expenses of Undergraduate Universities Affiliated with Liaoning Provincial Department (Grant Nos. LJ212410144051; LJ212410144032).

Institutional review board statement: Not applicable.

Informed consent statement: Not applicable.

Data availability statement: The data is unavailable due to privacy or ethical restrictions.

Conflict of interest: The authors declare no conflict of interest.

AI use statement: No AI tools were used for data analysis, interpretation, or generation of scientific content.

References

1. Zhao Y, Song Y, Zhou Z, et al. Fault diagnosis of air conditioning systems based on vibration features and multi-directional attention convolutional network. Energy and Buildings. 2026; 359: 117310. doi: 10.1016/j.enbuild.2026.117310
2. Wang S, Li X, Wang Y. Vibration Characteristics Analysis of multi-component Coupling Fault in Gear Transmission System. Journal of Vibration Engineering & Technologies. 2026; 14(4): 162. doi: 10.1007/s42417-026-02373-3
3. Xu M, Wang M, Zeng Y, et al. Dynamic modelling and vibration characteristic analysis of gear transmission system under the effect of time-varying misalignment from clearance of bearings. Measurement. 2026; 272: 120961. doi: 10.1016/j.measurement.2026.120961
4. Xing Z, Liu Y, Wang Q, et al. Vibration characteristics investigation of local defects in inter-shaft bearings considering time-varying load zones. Communications in Nonlinear Science and Numerical Simulation. 2026; 156: 109697. doi: 10.1016/j.cnsns.2026.109697
5. Yikun E, Feng Z, Liu Z, et al. Dynamic modeling and vibration analysis for cycloid gear bearing fault diagnosis of rotate vector reducers. Mechanical Systems and Signal Processing. 2026; 244: 113748. doi: 10.1016/j.ymssp.2025.113748
6. Wang S, Zhang M, Mo J. Contact-Vibration characteristics of TBM cutters with abnormal wear under multiple cutter and composite formation conditions. Tunnelling and Underground Space Technology. 2026; 167: 107051. doi: 10.1016/j.tust.2025.107051
7. Huang F, Wang Z, Chen C, et al. Vibration Characteristics of the Coupling Between Bearing Inner Ring Tilt and Rotor Angular Eccentricity Faults in Permanent Magnet Synchronous Motors. Journal of Vibration Engineering & Technologies. 2025; 13(7): 463. doi: 10.1007/s42417-025-02033-y
8. Hao Z, Wang D, Zhang Q, et al. Vibration characteristic analysis of a two-stage spur gear transmission system with tooth crack and profile shifted. Journal of Sound and Vibration. 2025; 615: 119211. doi: 10.1016/j.jsv.2025.119211
9. Chandan MN, Majumder H, Badadhe A. A Dual-Stream Gated Attention Network for Fault Diagnosis of Drill Bit Using Time and Frequency Domain-based Vibration Features. Journal of Vibration Engineering & Technologies. 2025; 13(8): 626. doi: 10.1007/s42417-025-02161-5
10. Chen D, Dai W, Yue L. Analysis of engine blade chipping fault based on vibration and stress testing fusion. Results in Engineering. 2025; 27: 105722. doi: 10.1016/j.rineng.2025.105722
11. Zhao Y, Lu Y, Han L, et al. Investigation Into the Axial Vibration Behaviour of Helical Windings With a Transposition Structure Under External Short-Circuit Faults. IET Electric Power Applications. 2025; 19(1): e70119. doi: 10.1049/elp2.70119
12. Xing Z, Guo C, Guo S. Vibration mechanism and characteristics analysis of oil-immersed transformer under multi-physical field coupling. Journal of Physics: Conference Series. 2025; 3110(1): 012014. doi: 10.1088/1742-6596/3110/1/012014
13. Ghorbel A, Bouaziz A, Feki N, et al. Vibration Monitoring of Flywheel Energy Storage System (FESS) in Presence of Gear Faults. Journal of Vibration Engineering & Technologies. 2025; 13(7): 493. doi: 10.1007/s42417-025-02069-0
14. Han W, Mu X, Liu Y, et al. A Critical Review of On-Line Oil Wear Debris Particle Detection Sensors. Journal of Marine Science and Engineering. 2023; 11(12): 2363. doi: 10.3390/jmse11122363
15. Yorston C, Chen C, Camelio J. Advancing architectural frameworks for vibration signature classification in rotating machinery. Proceedings of the Institution of Mechanical Engineers, Part B: Journal of Engineering Manufacture. 2025; 239(5): 711–725. doi: 10.1177/09544054241260928

16. Cao C, Li Z, Wang J, et al. Research on Simulation Analysis and Joint Diagnosis Algorithm of Transformer Core-Loosening Faults Based on Vibration Characteristics. Energies. 2025; 18(4): 914. doi: 10.3390/en18040914
17. Li S, Cui T, Jain A. Fusion-based intelligent decision method with factor code and factor pedigree in the system fault evolution process. Information Fusion. 2024; 108: 102354. doi: 10.1016/j.inffus.2024.102354
18. Li S, Cui T. Effect Analysis of Factors and Time on SFEP Using Multimodal Streaming Data under Uncertain Conditions. Tsinghua Science and Technology. 2025. doi: 10.26599/TST.2024.9010156
19. Guang C, Yan X, Zhang S, et al. Dynamic active torque coordination strategy for torsional vibration suppression in wind turbines during grid fault recovery. International Journal of Electrical Power & Energy Systems. 2026; 175: 111590. doi: 10.1016/j.ijepes.2026.111590
20. Deng K, Luo M, Yu Y, et al. Analysis of vibration characteristics of axle-box bearings in urban rail vehicles under internal and external excitation coupling. Vehicle System Dynamics. 2025, 63(11): 2185–2212. doi: 10.1080/00423114.2024.2403552
21. Yang DY, Huang JL, Zhu WD. Investigation on vibration characteristics of a rotor system with combined misalignment and eccentric faults under foundation swinging motion: Theoretical and experimental analyses. Mechanical Systems and Signal Processing. 2025; 240: 113332. doi: 10.1016/j.ymssp.2025.113332
22. Chen J, Zhang P, Li S, et al. Study on fault vibration characteristics of shield cutters based on FEM-MBD. Scientific Reports. 2025; 15(1): 37834. doi: 10.1038/s41598-025-21723-x
23. Liu K, Wang D, Chen B, et al. Vibration characteristics investigation of a single/dual rotor-bearing-casing system with local bearing defects. Mechanical Systems and Signal Processing. 2025; 225: 112227. doi: 10.1016/j.ymssp.2024.112227
24. Cui T, Li S. Research on basic theory of space fault network and system fault evolution process. Neural Computing and Applications. 2020; 32(6): 1725–1744. doi: 10.1007/s00521-019-04247-0
25. Olejnik P, Desta YD. Phenomenological friction modulation and near-field acoustic signatures in a slender post-buckled beam with rolling–stick–slip contact. Journal of Sound and Vibration. 2026; 627: 119661. doi: 10.1016/j.jsv.2026.119661
26. Beniwal R, Kalra S. Artificial neural network and acoustic emission-based fault diagnosis for wide temperature range silicon carbide MOSFET application. Semiconductor Science and Technology. 2026; 41(1): 015023. doi: 10.1088/1361-6641/ae2b9d
27. Rigolli D, Pompei L, Manfredini M, et al. The Development of a Predictive Maintenance System for Gearboxes Through a Statistical Diagnostic Analysis of Lubricating Oil and Artificial Intelligence. Machines. 2025; 13(8): 693. doi: 10.3390/machines13080693
28. Williamson K, Golay PA, Guiffrida F, et al. A rapid, solvent-free approach for detecting adulteration of vegetable oils using a single diagnostic region with low field NMR. Journal of Food Composition and Analysis. 2025; 144: 107726. doi: 10.1016/j.jfca.2025.107726
29. Wang Z, Lei XW, Guan X, et al. Reliability Assessment Method for Fault State Simulation Data in Diagnostic Models. Manufacturing Automation. 2024, 46(9): 179–183. (in Chinese)
30. Zhang J, Zhao Y, Liu M, et al. Reliability Modelling for Degradation Based on Type-II Generalized Logistic Distribution and Particle Swarm Optimization. Journal of South China University of Technology(Natural Science Edition), 2019, 47(5): 96–102. (in Chinese)
31. Ji MH. Research on Gear Transmission Fault Diagnosis Based on Numerical Simulation and Deep Transfer Learning. China University of Mining and Technology; 2024. (in Chinese)
32. Cao R. Research on Fault Simulation and Diagnosis Technology of Tapered Roller Bearings Based on Virtual Simulation [Master's Thesis]. Dalian Maritime University; 2024. (in Chinese)
33. Lv DX, Zuo YF, Fan MY, et al. Bearing fault data simulation generation method with characteristics of strong interference background noise. Journal of Mechanical & Electrical Engineering. 2024; 41 (11): 1923–1934. (in Chinese)
34. Paris P, Erdogan F. A Critical Analysis of Crack Propagation Laws. Journal of Basic Engineering. 1963; 85(4): 528–533. doi: 10.1115/1.3656900
35. Liu S, Dong Y, Qiao Y, et al. Research on Dynamic Fault Injection of Bearing Digital Twin Model Based on Improved Dung Beetle Optimization Algorithm. Journal of Mechanical Engineering. 2026; 62(3): 446–457. (in Chinese)